

# Formation of Silver Nanoparticles and Self-Assembled Two-Dimensional Ordered Superlattice

Shengtai He,<sup>†</sup> Jiannian Yao,<sup>‡</sup> Peng Jiang,<sup>†</sup> Dongxia Shi,<sup>†</sup> Haoxu Zhang,<sup>†</sup>  
Sishen Xie,<sup>†</sup> Shijin Pang,<sup>†</sup> and Hongjun Gao<sup>\*,†</sup>

Beijing Laboratory of Vacuum Physics, Institute of Physics & Center for Condensed Matter Physics, Chinese Academy of Sciences, Beijing 100080, China, and Institute of Chemistry & Center for Molecular Sciences, Chinese Academy of Sciences, Beijing 100101, China

Received August 28, 2000. In Final Form: December 11, 2000

1-Nonanethiol-capped silver nanoparticles of about 4.18 nm in diameter were prepared using a liquid–liquid two-phase method. Two-dimensional ordered superlattices of the nanoparticles were formed on carbon films coated on transmission electron microscopy (TEM) copper grids by evaporating a drop of the dispersion in chloroform. The formation process of the silver nanoparticles was investigated by UV–visible absorption spectroscopy and TEM. A blue shift of the maximum absorption peak position of the UV–vis spectra occurred at the beginning of the reaction, followed by a red shift. This result indicated that large thiol-capped silver nanoparticles were formed at the beginning, then the large particles were decomposed into small particles, and in the final stage the small particles enlarged slightly again. The TEM images show directly the same process with the results from the UV–vis spectra. In addition, the UV–visible spectra of the silver nanoparticle colloidal phase obtained finally show that the system is monodisperse and can remain stable for several weeks.

## Introduction

The study of nanoparticles of noble metals has been an extremely active area in recent years because of their interesting properties which are different from those of bulk substances.<sup>1–12</sup> In the past few years, many investigations have been focused on the control of the size of nanocrystals and their self-assembly into two-dimensional (2D) (or three-dimensional (3D)) superlattice structures.<sup>13</sup> Using colloidal metal or semiconductor nanoparticles as building blocks to construct ordered mesoscopic structural materials will provide the possibility of detecting the collective physical properties of the ensemble and further exploring size-tunable optical and electronic properties of the nanocrystals in devices such as single electron transistors. To prepare the small particles at nanometer scale and their ordered 2D structures, capped organic molecules such as alkylthiol are necessary for preventing

the nanoparticles from irreversible aggregation in a solvent and making the particles soluble in given solvents. In addition, a tight size distribution is also required for the superlattice formation. Thus, the study of the nanoparticle formation process is crucial not only for understanding the particle growth but also for controlling the size distribution. However, less attention has been paid on this research project. Recently, Chen et al. examined the evolution of the core of hexanethiolate monolayer protected Au clusters at time intervals of 125 h<sup>14</sup> and the growth of alkanethiolate-protected palladium nanoparticles.<sup>15</sup> Patel and co-workers<sup>7</sup> reported the formation of silver clusters and nanoparticles prepared in polyacrylate and inverse micellar solutions. In this paper, we will present the particle formation process based on the maximum absorption wavelength of the 1-nonanethiol-capped silver nanocrystals and the evolution of their core sizes in chloroform using UV–visible absorption spectroscopy. Transmission electron microscopy (TEM) was employed to characterize the nanoparticle formation. It was found that the TEM results are consistent with the results from the UV–visible spectra.

## Experimental Section

**Nanocrystal Synthesis.** Silver nitrate (AgNO<sub>3</sub>) and sodium borohydride (NaBH<sub>4</sub>) were obtained from Acros. Tetra-*n*-octylammonium ((C<sub>8</sub>H<sub>17</sub>)<sub>4</sub>NBr) was obtained from Tokyo Chemical Co. 1-Nonanethiol (CH<sub>3</sub>(CH<sub>2</sub>)<sub>8</sub>SH) and other reagents were supplied by Aldrich. All the reagents were used as received, without further purification, and all the water was deionized. Silver nanoparticles were prepared according to ref 16. Thirty milliliters of an aqueous silver ion solution (0.03 M AgNO<sub>3</sub>) was mixed with 20 mL of a chloroformic solution of phase transfer catalyst (0.20 M (C<sub>8</sub>H<sub>17</sub>)<sub>4</sub>NBr) and stirred vigorously for 1 h. The French gray organic phase was subsequently collected, and 150 μL 1-nonanethiol was added. After the nonanethiol/Ag<sup>+</sup> solution

<sup>†</sup> Institute of Physics & Center for Condensed Matter Physics, Chinese Academy of Sciences.

<sup>‡</sup> Institute of Chemistry & Center for Molecular Sciences, Chinese Academy of Sciences.

- (1) Hanamura, E. *Phys. Rev. B* **1988**, *37*, 1273.
- (2) Ozin, G. A. *Adv. Mater.* **1993**, *5*, 412.
- (3) Duff, D. G.; Baiker, A. *Langmuir* **1993**, *9*, 2301.
- (4) Aihara, N.; Torigoe, K.; Esumi, K. *Langmuir* **1998**, *14*, 4945.
- (5) Plieni, M. P.; Taleb, A.; Petit, C. *J. Dispersion Sci. Technol.* **1998**, *19* (2 and 3), 185.
- (6) Bright, R. B.; Musick, M. D.; Natan, M. J. *Langmuir* **1998**, *14*, 5695.
- (7) Zhang, Z.; Patel, R. C.; Kothari, R.; Johnson, C. P.; Friberg, S. E.; Aikens, P. A. *J. Phys. Chem. B* **2000**, *104*, 1176.
- (8) Wang, W.; Efrima, S.; Regev, O. *Langmuir* **1998**, *14*, 602.
- (9) Liz-Marzan, L. M.; Lado-Tourino, I. *Langmuir* **1996**, *12*, 3585.
- (10) Matejka, P.; Vlckova, B.; Vohidal, J.; Pancoska, P.; Baumrunk, V. *J. Phys. Chem.* **1992**, *96*, 1361.
- (11) Sun, T.; Seff, K. *Chem. Rev.* **1994**, *94*, 857.
- (12) Mostafavi, M.; Marignier, J. L.; Amblard, J.; Belloni, J. *Radiat. Phys. Chem.* **1989**, *34*, 605.
- (13) (a) Giersig, M.; Mulvaney, P. *Langmuir* **1993**, *9*, 3408. (b) Mirkin, C. A.; Letsinger, R. L.; Mucic, R. C.; Storhoff, J. J. *Nature* **1996**, *382*, 609. (c) Feldstein, M. J.; Keating, C. D.; Liao, Y. H.; Natan, M. J.; Sherer, N. F. *J. Am. Chem. Soc.* **1997**, *119*, 6638. (d) Andres, R. P.; Bielefeld, J. D.; Henderson, J. I.; James, D. B.; Kolagunta, V. R.; Kubiak, C. P.; Mahoney, W. J.; Osifchin, R. G. *Science* **1996**, *273*, 1690.

(14) Chen, S.; Templeton, A. C.; Murray, R. W. *Langmuir* **2000**, *16*, 3543.

(15) Chen, S.; Huang, K.; Stearns, J. A. *Chem. Mater.* **2000**, *12*, 540.  
(16) Brust, B.; Walker, M.; Bethell, D.; Schiffrin, D. J.; Whyman, R. *J. Chem. Soc., Chem. Commun.* **1994**, 801.

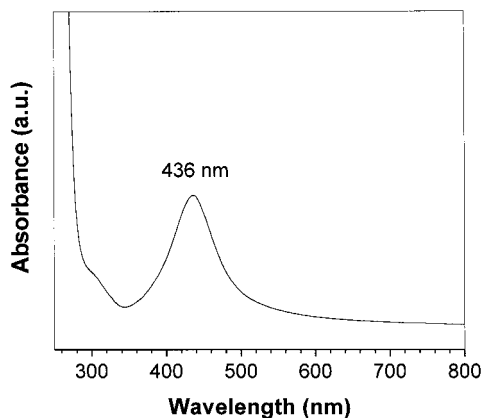


**Figure 1.** Typical UV-vis spectrum of the silver nanoparticles capped by 1-nonanethiol.

was stirred for 15 min, 24 mL of fresh aqueous sodium borohydride (0.43 M NaBH<sub>4</sub>) solution used as the reducing agent was injected, and the system color became sable immediately. The reaction mixture was stirred for over 3 h before the organic/nanocrystal-rich phase was collected. It is possible to form AgBr during the reaction; however, the effect of the formed AgBr is so small that it can be ignored in the following discussion. The dispersion phase was washed three times with ethanol to remove the phase transfer catalyst, excess 1-nonanethiol, and reaction byproducts. The final product is the silver nanoparticle organosol.

**Experimental Techniques.** UV-visible absorption spectra of nanocrystal dispersions in chloroform were measured using a Shimadzu UV-1601 PC double beam spectrophotometer. All the samples for the measurements of UV-vis spectra were diluted except for the samples used to investigate the changes of the UV-vis spectra during the nanoparticle formation. Transmission electron micrographs were obtained from a JEM 200CX operating at 200 kV. IR spectra were recorded using a Mattson Galaxy 3000 FT spectrometer at room temperature by dropping the samples on the KBr windows. The size distribution was derived from a histogram which was obtained by measuring the diameter of all the particles from different parts of the grid; about 400 particles were taken into account to establish the histogram. The full width at half-maximum (fwhm) values of the UV-vis spectra were measured from the following steps. First, a line was drawn by linking the top point of the peak to the center of the baseline, then a line which is parallel to the baseline was made through the center of the resulting line. After that, there are two points of intersection between the line and the peak. The wavelength difference between the two points is just the fwhm value of the absorption peak.

**Superlattice Formation.** An ordered array of 1-nonanethiol-capped silver nanocrystals was formed by evaporating the solvent from a dispersion on a carbon film coated on copper grids at room temperature. A layer of carbon film was first coated on the surface of mica by vacuum evaporation, and then the mica wafer was dipped into water to make the carbon film separate from the surface of the mica and float on the water. A drop of the silver dispersion was deposited on the floating carbon film. After the solvent evaporated, a TEM copper grid was placed in the water and lifted through the interface at a constant surface pressure and constant speed. Finally, the nanoparticle-modified carbon film was transferred onto the grid.

## Results and Discussion

**The Superlattice of Silver Nanoparticles.** Figure 1 is a typical UV-vis spectrum of a 1-nonanethiol-capped silver colloid suspension in chloroform, in which the extinction band for silver nanoparticles appears at 436 nm with a fwhm of 80 nm. This is the characteristic of rather monodisperse thiol-capped silver nanoparticles,<sup>17</sup> whereas uncapped silver colloids exhibit absorption with a maximum at 390 nm. The large shift of the maximum absorption wavelength ( $\lambda_{\text{max}}$ ) can be ascribed to the bond formation of the S ions and the Ag atoms of the nano-

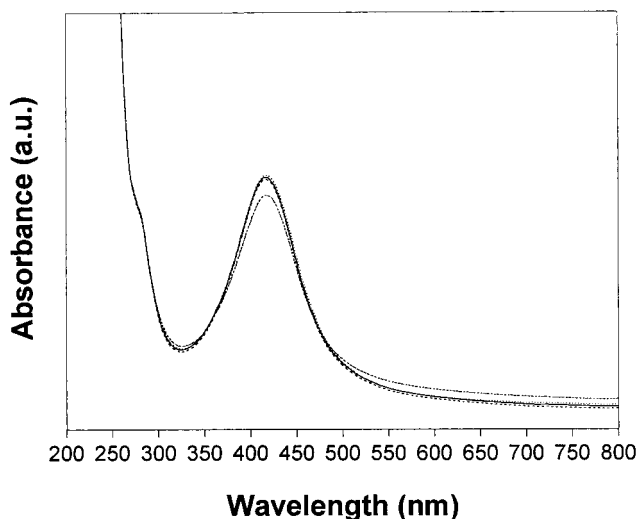


**Figure 2.** UV-vis spectra of the silver nanocrystals stored at different times: (dotted line) 1 week, (dashed line) 2 weeks, (solid line) 3 weeks, and (dashed-dotted line) 4 weeks.

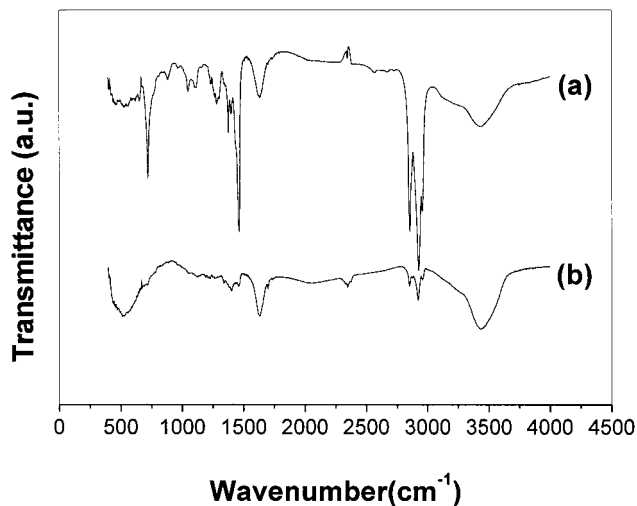


**Figure 3.** IR spectra of free 1-nonanethiol (a) and the particles capped by 1-nonanethiol (b).

particle. This shift of the absorption band provides clear evidence for the adsorption of the 1-nonanethiol on the silver particles.<sup>18</sup> The good symmetric absorption peaks with a nearly unchanged width imply that the size of the nanoparticles is very uniform, which does not depend on the silver concentration.

To detect the stability of the 1-nonanethiol-protected silver nanoparticles in chloroform, we measured the absorption spectra of one of the colloid systems with the same concentration at different times. As shown from Figure 2, there is no obvious difference in the shape, position, and symmetry of the absorption peak during the initial 3 weeks. After the fourth week, the fwhm of the spectrum starts to become wider than before, and the position of the peak has a slight red shift, implying the onset of nanoparticle aggregation. These spectra demonstrate that the silver nanoparticle colloidal solution can remain stable for about 1 month. It can be seen in our discussion above that there is a symmetry difference in the spectra of the surface plasmon band between the nanoparticles that are uniform and those that are

(17) Creighton, J. A.; Eaton, D. G. *J. Chem. Soc., Faraday Trans. 1991*, 87, 3881.

(18) Kerker, M. *J. Colloid Interface Sci.* **1985**, 105, 297.

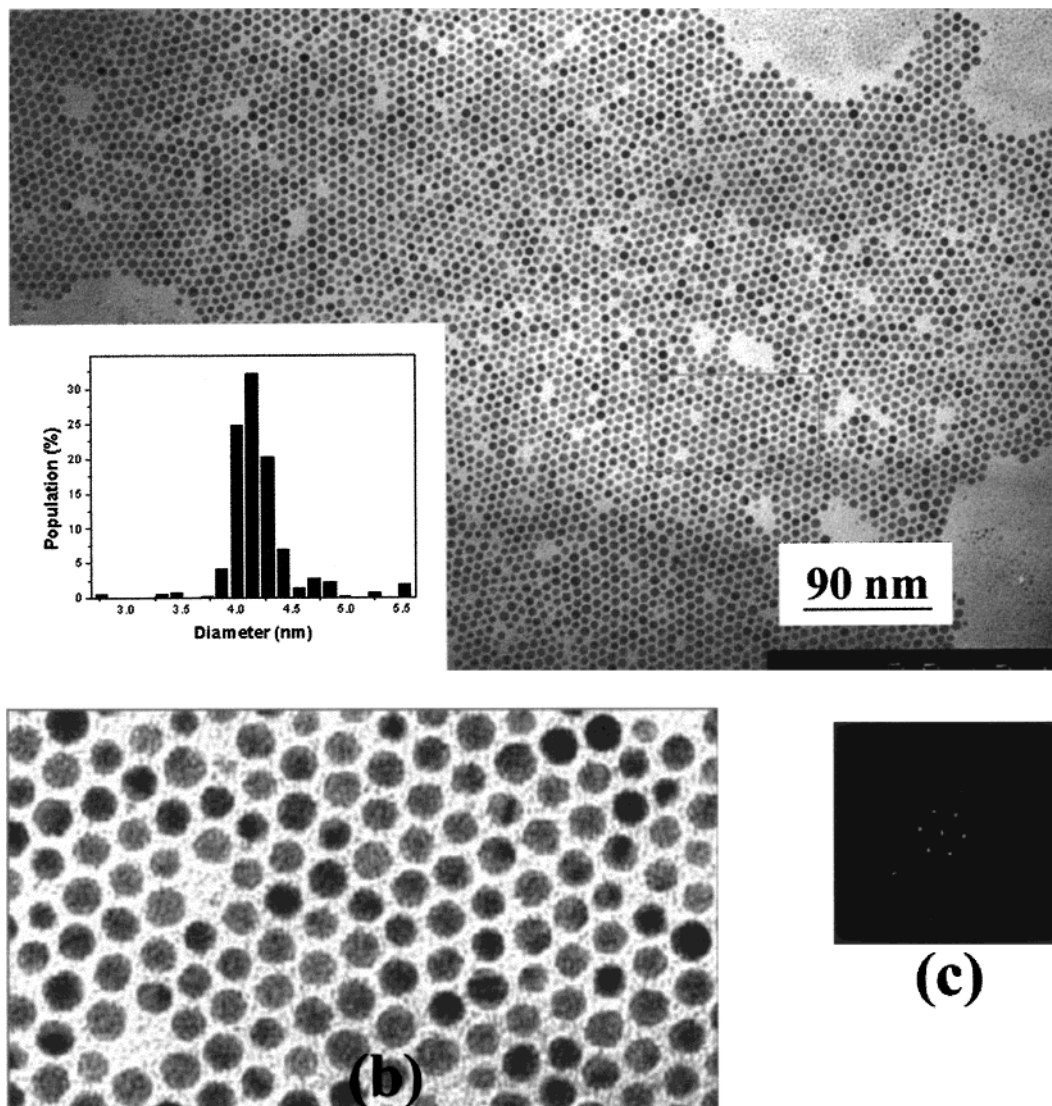


**Figure 4.** (a) TEM image of a two-dimensional silver nanoparticle superlattice and (inset) the histogram of the nanoparticles. (b) TEM image of the selected area in (a). (c) The 2-D Fourier transform power spectrum of the image in (b).

nonuniform in size, which is due to the size distribution of the nanoparticles.

The IR spectra of the free 1-nonanethiol and the particles capped by 1-nonanethiol are given in Figure 3. The IR spectra of the nanoparticles and the free 1-nonanethiol molecule are similar to one another, indicating that the organic molecules have indeed become a part of the nanoparticles. However, a remarkable difference in the peak intensity is found between the peaks in parts a and b of Figure 3. Those peaks correspond to the C–S stretching mode ( $\nu_{C-S} = 718 \text{ cm}^{-1}$ ), the in-plane rocking mode of the terminal methyl group ( $\rho_{CH_3} = 1025 \text{ cm}^{-1}$ ), and the non-in-plane rocking mode and the wagging mode of the methylene group ( $\omega_{CH_2} = 1270 \text{ cm}^{-1}$  and  $\delta_{CH_2} = 1455 \text{ cm}^{-1}$ , respectively). The reason for the intensity difference between the two spectra is believed to be that the thiolate molecules on the nanoparticle form a relatively close-packed thiol layer and molecular motion is constrained.<sup>19,20</sup> Thus, this steric constraining effect on the transverse mode (rocking mode, wagging mode, etc.) is stronger than that on the longitudinal mode (stretching mode, etc.). Therefore,

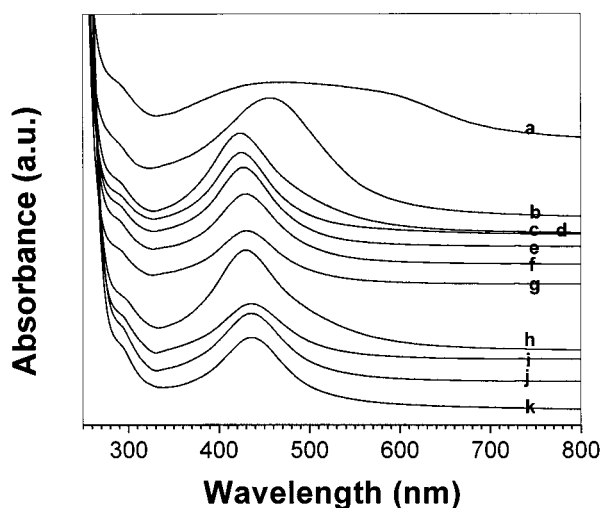
the change of the peak intensity of the longitudinal modes is smaller than that of the transverse mode. The longitudinal modes are the asymmetric and symmetric methylene stretching modes and the asymmetric in-plane and symmetric stretching modes of the terminal methyl groups, whose peak positions are nearly in the range from  $2700$  to  $3000 \text{ cm}^{-1}$ . The C–S stretching mode is due to the position of the C–S bond nearest to the surface of the silver particle, and a chemical bond can be formed between S ions and Ag atoms.

Figure 4 is a TEM picture and shows the size distribution of the silver nanoparticles. Figure 4a is a low-resolution TEM image. For clarity, we zoom in on Figure 4a and highlight the crystallographic structure of the phase, as shown in Figure 4b. Figure 4c is the 2-D Fourier transform power spectrum of the image in Figure 4b, which further confirms the hexagonal close-packed (hcp) superlattice. From the histogram of the size distribution in Figure 4a (inset), we find that the standard deviation of the size distribution is 0.23. Figure 4a also demonstrates that the mean diameter of the nanoparticles is 4.18 nm, which has just fallen into the size range exhibiting quantum size effects, and the average interparticle spacing is 1.51 nm. The ordered domains in the monolayer typically extend over an area of  $0.5 \mu\text{m} \times 0.5 \mu\text{m}$ . They are usually separated

(19) Ulman, A. *An Introduction to Ultrathin Organic Films: from Langmuir-Blodgett to Self-assembly*; Academic Press: Boston, 1991.

(20) Korgel, B. A.; Fullam, S.; Connolly, S.; Fitzmaurice, D. *J. Phys. Chem. B* **1998**, *102*, 8379.





**Figure 5.** UV-visible spectra of the silver particles at different times during the reaction: (a) 0 min, (b) 15 min, (c) 30 min, (d) 45 min, (e) 60 min, (f) 75 min, (g) 90 min, (h) 105 min, (i) 120 min, (j) 135 min, and (k) 150 min.

by domain boundaries resulting from the solvent evaporation rate and the rough surface morphology and the defects on the surface of the substrate.

**The Study of Silver Nanoparticles' Formation.** The formation process of 1-nonanethiol-modified silver nanoparticles was traced by the UV-visible absorption method. Figure 5 shows the shifts of the peak positions and the shapes of the absorption spectra during the whole reaction process at time intervals of 15 min. When the injection of the reducing agent ( $\text{NaBH}_4$ ) was finished, a very broad UV-visible band (see Figure 5a) appeared, which is very similar to the solution absorption spectrum before the reducing agent was added, showing that the particles were not formed at that time. When the reaction continued, a remarkable peak appeared and the peak position changed from 457 nm at 15 min to 424 nm at 30 min, as seen in Figure 5b,c. From this result, one can see the particle formation process at this stage: large particles were formed at the beginning of the reaction, and then the large particles decomposed to small ones. Later on, the position change of the corresponding peaks did not keep the blue shift but rather turned to the red shift, from 425 nm at 45 min to 436 nm at 120 min (see Figure 5d-i). This result indicates that the particle size became larger and larger with time in the reaction. However, the red-shift value of 12 nm is much smaller than the 33 nm of the blue shift at the beginning of the reaction. The position of the peak did not change and remained at 436 nm when the reaction time was up to 120 min, as shown in Figure 5j,k. At the same time, from the shape of the absorption peak we can also acquire information on the changes of the size distribution. As we know, when the solution system is monodisperse (narrow size distribution) the peak shape is symmetric and the value of the fwhm is small. When the system is polydisperse, the peak shape is asymmetric, which suggests that the peak actually consists of two or more absorption peaks.<sup>21,22</sup> From Figure 5, we find that the peak shape changed visibly from asymmetric to symmetric, and the peak became narrower because of the decrease of the corresponding fwhm values from 130 to 80 nm during the reaction. Those results mean that the size distribution becomes narrower, and the colloid system

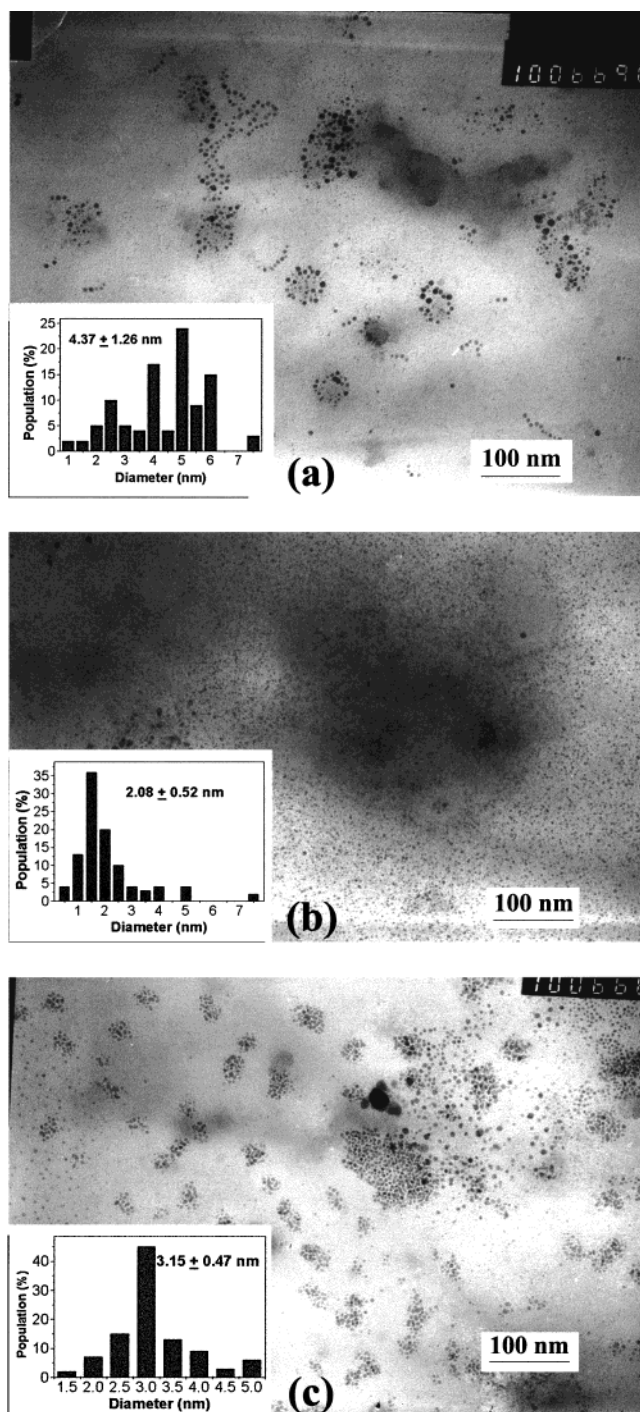


**Figure 6.** TEM micrographs of capped silver particles and (insets) the corresponding size histograms at different reaction times: (a) 15 min, (b) 30 min, and (c) 60 min.

changes from polydispersion to monodispersion. This phenomenon can also be seen in the following TEM results.

Figure 6 shows TEM micrographs of the thiol-capped silver particles at different reaction times. Figure 6 shows that the particles were quite big, in the range of  $4.37 \pm 1.26$  nm, and the size distribution was broad at the initial time of 15 min. However, at 30 min the particle size strongly decreased to  $2.08 \pm 0.52$  nm, and at 1 h the size of the particles slowly increased to  $3.15 \pm 0.47$  nm, when the particles were more uniform than those at the initial time of 15 min.

In fact, as mentioned in the Experimental Section the color change can also show the size change process of the

(21) Brown, K. R.; Walter, D. G.; Natan, M. J. *Chem. Mater.* **2000**, *12*, 306.

(22) Bohren, C. F.; Huffman, D. R. *Absorption and Scattering of Light by Small Particles*; John Wiley & Sons: New York, 1983.

nanoparticles. When sodium borohydride solution was added to the nonanethiol/Ag<sup>+</sup> mixture, the color of the solution changed quickly from French gray to sable or black, which indicates the formation of silver particles.<sup>14</sup> Then, the color gradually changed to orange while the mixture was stirred for 120 min at room temperature, suggesting that the initially produced particles were not stable and were decomposed to small particles. Thus, the growth process of the silver nanoparticles capped by 1-nonanethiol can be summarized into the following stages. (1) During the first 15 min, large particles were formed in a rapid nucleation process. (2) The large particles were rapidly decomposed into small particles in the following 15 min. (3) A longer time (90 min) was required for a slight increase of the core size after the big particles decomposed into smaller ones. In addition, during the whole formation process of the nanoparticles the system changed from a phase that was polydisperse in size to one that was monodisperse in size. Thus, during the formation process of the nanoparticles the particle size distribution becomes narrow.

It is of interest to know the formation process of the nanoparticle. From these limited experimental data, it is hard to give detailed information on the process. However, based on our experimental results we can roughly elucidate this growth process as follows. At the beginning of the reaction, silver ions were reduced to atoms from the solution at a very short time just after the reduction solution was added. The Ag atoms aggregated rapidly together to form small nanoparticles, and then the formed small nanoparticles soon aggregated to become large nanoparticles because of the high density of the small nanoparticles. In the process of the aggregation, there is less capping agent adsorbed on the particles. This is a nonequilibrium process. The formed large particles are not stable. The large nanoparticle will be broken into small parts because of the fact that the 1-nonanethiol prevalently links the surface of Ag nanoparticles, which can make the small nanoparticles separate from the large nanoparticles. This reaction goes on, and more silver ions

are reduced to silver atoms. Finally, the particle size stops decreasing and starts to increase at a certain reaction moment. The whole process is a dynamic one; that is, during the increase of the particle size there are some larger particles to decompose into smaller nanoparticles. This is also true for the reverse process. This can be the key to understanding why the standard deviation decreases with the reaction. However, more work on the experiment and theory should be explored to understand in detail the formation process of the nanoparticle.

### Conclusions

1-Nonanethiol-capped silver nanoparticles were prepared employing the two-phase liquid-liquid system method. The IR spectra showed that the 1-nonanethiol was a part of the nanoparticles, and the UV-vis spectrum of the colloidal silver particles in chloroform shows the system was size monodisperse and stable, which is key to obtaining the ordered lattice. The long-range ordering of close-packed nanoparticle arrays, as confirmed by TEM, was obtained by the self-assembly technique.

With the UV-vis absorption spectrum, the formation process of the nanoparticles was investigated and discussed. Following the initial blue shift from 457 to 424 nm, the maximum absorption peak positions of the UV-visible spectra were observed to shift to the low-energy side from 424 to 436 nm. The peak shape changes from asymmetric to symmetric. All of these results indicated that large particles were rapidly formed at the initial stage, then the large particles decomposed into small particles, and at the final stage the small particles grew slightly. Meanwhile, during the reaction the system changed from a polydispersion phase to a monodispersion phase. However, more work on the experiment and the theory is needed to further understand the formation mechanism.

**Acknowledgment.** The authors thank B. S. Zhou for helpful discussions. This work was supported in part by the Natural Science Foundation of China.

LA001239W